Article

Surface Functionalization of PEO Nanofibers Using a TiO_2 Suspension as Sheath Fluid in a Modified Coaxial Electrospinning Process

ZHENG Gaofeng[1,2]✉, PENG Hao[1,2], JIANG Jiaxin[1,2], KANG Guoyi[1,2], LIU Juan[1,2], ZHENG Jianyi[1,2] and LIU Yifang[1,2]✉

Received March 15, 2021
Accepted April 14, 2021

Convenient and integration fabrication process is a key issue for the application of functional nanofibers. A surface functionalization method was developed based on coaxial electrospinning to produce ultraviolet(UV) protection nanofibers. The titanium dioxide(TiO_2) nanoparticles suspension was delivered through the shell channel of the coaxial spinneret, by which the aggregation of TiO_2 nanoparticles was overcome and the distribution uniformity on the surface of polyethylene oxide(PEO) nanofiber was obtained. With the content of TiO_2 increasing from 0 to 3%(mass fraction), the average diameter of nanofibers increased from (380± 30) nm to (480±100) nm. The surface functionalization can be realized during the electrospinning process to gain PEO/TiO_2 composite nanofibers directly. The uniform distribution of TiO_2 nanoparticles on the surface of nanofibers enhanced the UV absorption and resistance performance. The maximum UV protection factor(UPF) value of composite nanofibers reaches 2751. This work presented a novel surface-functionalized way for the preparation of composite nanofiber, which has great application potential in the field of micro/nano system integration fabrication.

Keywords Coaxial electrospinning; Surface functionalization; TiO_2 nanoparticle; Composite nanofiber; UV protection

1 Introduction

UV radiation is harmful to human body. Long-term UV exposure to radiation will cause skin redness, itching, darkening and even skin cancer[1−4]. UV radiation causes physical and chemical changes inside materials and accelerates the aging of rubber and plastic products, resulting in photo-degradation and photo-aging, thus the service life of products is reduced[5−8]. Therefore, the development of a breathable and anti-UV material has great application prospects.

In the past decades, electrospinning technology has gained widespread attention for its ability to produce nano-scale fibers with a large specific surface area at low cost and its controllable process. The introduction of functional materials in the electrospinning process is a popular method to enhance the properties of nanofibrous membrane, such as mechanical[9,10], physical[11,12], chemical[13], catalytic[14,15] and other properties. With its advantages of good UV resistance, self-cleaning ability, antibacterial and oxidation properties[16—18], TiO_2 has been a very promising candidate in the fields of spinning, cosmetics, coatings, sensors, etc.

TiO_2 nanoparticles have been demonstrated to be suitable for the preparation of multifunctional composite nanofibers through electrospinning[19]. Lee *et al*.[20] prepared PVA/TiO_2 nanocomposite fiber webs by electrospinning, and assessed their UV protection properties, antibacterial functions, formaldehyde decomposition ability, and ammonia deodorization efficiency. Yu *et al*.[21] used a one-step *in situ* polymerization method to co-dope TiO_2, sulfosalicylic(SSA), sodium dodecyl benzene sulfonate(SDBS) with polyaniline (PANI). Lu *et al*.[22] converted the precursor to TiO_2 by calcination to obtain photovoltaic nanofiber. Due to the effect of van der Waals forces, nanoparticles agglomerate easily during the fabrication process, which reduces the properties of functional nanofiber[23−25]. Meanwhile, the post process, which is essential for hybrid solution electrospinning to fabricate functional nanofiber causes damage to the micro/nano structure and tends to cause material waste.

Coaxial electrospinning was initially thought to be successfully implemented only when the sheath fluid was electrospinnable[26]. Most recently, several publications demonstrated that solvent[27], unspinnable dilute polymer solution[28], solutions containing little molecules[29] can be utilized as an outer fluid to carry out modified coaxial and also tri-axial processes. However, no reports have tried an unspinnable nano suspension as a sheath fluid to carry out the modified coaxial process.

A surface-functionalized method based on a modified coaxial electrospinning process was presented in this work to prepare composite PEO/TiO_2 nanofibers for UV protection. The TiO_2 nanoparticles suspension was delivered through the shell channel of coaxial spinneret, by which the aggregation of

✉ ZHENG Gaofeng
zheng_gf@xmu.edu.cn
✉ LIU Yifang
yfliu@xmu.edu.cn
1. Department of Instrumental and Electrical Engineering, Xiamen University, Xiamen 361102, P. R. China
2. Fujian Innovation Center of Additive Manufacturing, Fuzhou 350118, P. R. China

https://doi.org/10.1007/s40242-021-1118-2

TiO_2 nanoparticles was overcome and the distribution uniformity of the nanoparticles on the surface of PEO nanofiber was enhanced. The composite PEO/TiO_2 membrane had excellent shielding effect on UV light. The fabrication process, element distribution characteristics, and UV resistance performance of the composite PEO/TiO_2 nanofiber were studied.

2 Experimental

2.1 Materials

PEO(M_w=300000) was purchased from Changchun Earth Fine Chemical Co., Ltd.(Changchun, China). TiO_2 nanoparticles (diameter of particles of 100 nm) were bought from Shanghai Macklin Biochemical Co., Ltd.(Shanghai, China). Ethanol (C_2H_5OH, ≥99.7%) was purchased from Sinopharm Chemical Reagent Co., Ltd.(Shanghai, China).

2.2 Fabrication of Electrospinning PEO/TiO_2 Nanofiber Membranes

The electrospinning process for the preparation of composite nanofibers is illustrated in Fig.1. The mixed solvent of deionized water and ethanol(volume ratio 1:3) was used to prepare an electrospinning solution, which was loaded to the core channel of the coaxial spinneret. The mass fraction of PEO in the solution was 8%. The mass fractions of TiO_2 nanoparticles in the solution was 0 and 1%, respectively. The solution was stirred overnight at 60 °C to achieve the homogeneous solution. The TiO_2 nanoparticles suspension in ethanol was loaded to the shell channel. The mass fractions of TiO_2 nanoparticles in the suspension were 0.5%, 1%, 2% and 3%, respectively. The suspension was ultrasound-treated for 30 min before experiments. The TiO_2 suspension surrounded the core solution jet and the TiO_2 nanoparticles were dispersed evenly on the surface of nanofiber.

Then, several groups of solutions with different solution ratios were used to investigate the process characteristics, as listed in Table 1. An integrated electrospinning equipment (NLM-0001, Xiamen Narai Technology Co., Ltd., Xiamen, China) was used to conduct the electrospinning experiment. The diameters of the core channel and the shell channel of the coaxial spinneret were 0.4 and 1.0 mm, respectively. The solution was delivered to the core channel and the shell channel by two precision syringe pumps(Pump 11 Pico Plus Elite, Harvard Apparatus America, USA) with flow rates of 300 and 100 μL/h, respectively. A conductive substrate was put on the *X*-*Y* motion platform to collect electrospun nanofiber. The distance between the needle tip and the collector was 15 cm. The reciprocating movement of the motion platform was controlled by a host computer to gain a uniform nanofibrous membrane. The velocity of the motion patform was 60 mm/s. A high voltage in the range of 10—15 kV was applied to stretch the solution into Taylor cone and fine jet by the the high

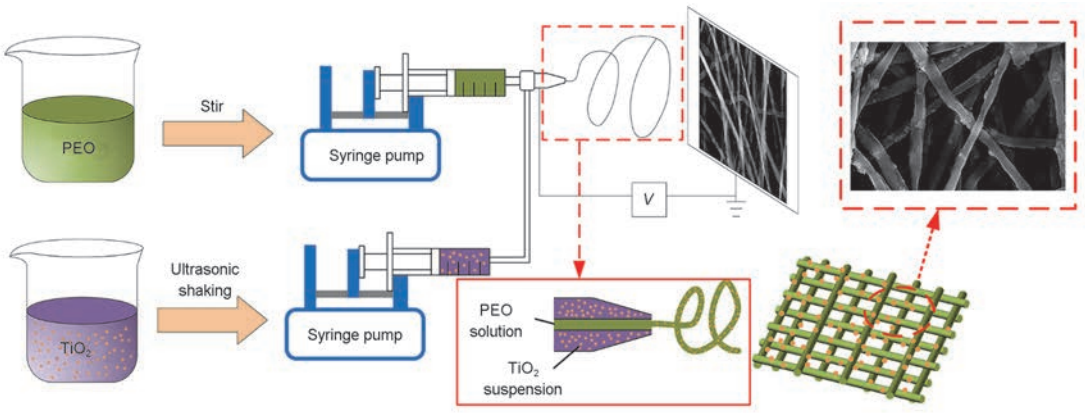

Fig.1 Schematic diagram of the surface functionalization method by coaxial electrospinning

Table 1 Components of the nanofibers produced by coaxial electrospinning techniques

Sample	Core	Shell
P	8% PEO	—
P-$T^{0.5}$	8% PEO+0.5% TiO_2 mixed solution	—
P-T^1	8% PEO+1% TiO_2 mixed solution	—
P/T^1	8% PEO	1% TiO_2 suspension
P/T^2	8% PEO	2% TiO_2 suspension
P/T^3	8% PEO	3% TiO_2 suspension
P-T^1/T^1	8% PEO+1% TiO_2 mixed solution	1% TiO_2 suspension
P-T^1/T^2	8% PEO+1% TiO_2 mixed solution	2% TiO_2 suspension
P-T^1/T^3	8% PEO+1% TiO_2 mixed solution	3% TiO_2 suspension

https://doi.org/10.1007/s40242-021-1118-2

voltage source(DW-SA403-1ACE5, Dongwen High Voltage Power Source Ltd., Tianjin, China). And then, the electrospinning composite membranes were dried for 4 h at 40 °C *in vacuum* to remove the residual solvent. The collecting time of electrospun nanofiber was 150, 300, 450 and 600 s, then the thickness of composite nanofibrous membrane can be adjusted. All the experiments were carried out under ambient conditions.

2.3 Characterization of Electrospun Composite Nanofiber

The surface morphologies of the samples were observed on a field emission scanning electron microscope(SEM, Supar 55 Sapphire, Carl Zeiss Co. Ltd., Germany). All the samples were sputter-coated with gold film before observation. The nanofiber diameter distributions were analyzed by ImageJ through the SEM images.

The chemical composition was determined by using energy dispersive X-ray spectrometry(EDS, X-Max^N-80, Oxford Instruments Co., Ltd., Germany) for all the samples. Meanwhile, the spatial distributions of carbon(C), oxygen(O), titanium(Ti) were obtained by EDS mapping analysis.

The phase analyses of the nanofibers were taken on an X-ray diffraction(XRD) analyzer(XRD-7000, Shimadzu Co., Ltd., Japan, 2θ=10°—100°), with Cu $K\alpha$ radiation(λ=0.1540 nm) at a scanning rate of 10°/min.

Fourier transform infrared spectra(FTIR) were acquired by using an infrared spectrum analyzer(NICOET iS10, Thermo Fisher Scientific, U.S.) to observe the spectral absorption peaks of the fiber samples. The samples were cut into small pieces for the performance measuring.

2.4 Anti-UV Performance Measuring

A measuring equipment of anti-UV performance was designed, as shown in Fig.2. The measuring samples were placed on a transparent substrate. A UV light source(SHENYU V2) was utilized in this equipment. The UV intensity is quantified on a UV spectrophotometer(MOLECULAR DEVICES SpectraMax® CMax Plus). The transmitted UV light was measured to evaluate the anti-UV performance. The composite nanofibrous membranes were cut into 3 cm×3 cm size samples, and placed between the UV light and the UV photometer. The light with wavelengths of 360(UV-A) and 290 nm(UV-B) was used in the measuring process.

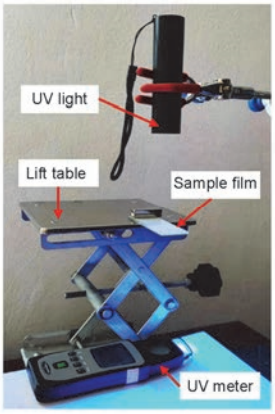

Fig.2 Anti-UV performance measuring equipment

2.5 UV Protection Tests

A fresh leaf(greenery) was placed under the UV lamp as shown in Fig.3(A). Samples of 1#, 2#, 3# and 4#(P, P-T^1, P/T^3 and P-T^1/T^3) were put on the same leaf, as shown in Fig.3(B). The UV intensity of the radiation on the leaf surface was 2000 μW/cm^2. The leaf surface under the UV light was recorded every 3 h.

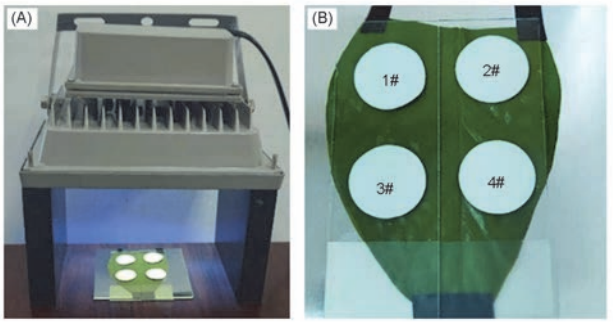

Fig.3 UV protection performance measuring
(A) Measuring equipment; (B) measuring sample on the green leaf.

3 Results and Discussion

3.1 Morphology and Diameter of Nanofibers

The SEM images and nanofiber diameter distributions of the nanofibrous membrane are shown in Fig.4. The surface of PEO nanofiber without TiO_2 nanoparticles was smooth. With the addition of TiO_2 nanoparticles, the surface of the fiber became rough, and the diameter of the nanofiber increased. The TiO_2 nanoparticles were observed to distribute evenly on the surface of nanofiber.

As the TiO_2 suspension was delivered separately through the shell channel, the aggregation of nanoparticles was overcome. There were more nanoparticles dispersed on the nanofiber surface of P/T^1 and P/T^3 than that of P-T^1, showing that delivering the dispersion solution in the shell channel was a simple and efficient method to reduce the aggregation and to increase the content of TiO_2 nanoparticles on the surface of composite nanofiber. At the same time, the shell dispersion was also a good method to promote the ejection of high viscous solution, and to avoid the blockage of electrospinning spinneret.

https://doi.org/10.1007/s40242-021-1118-2

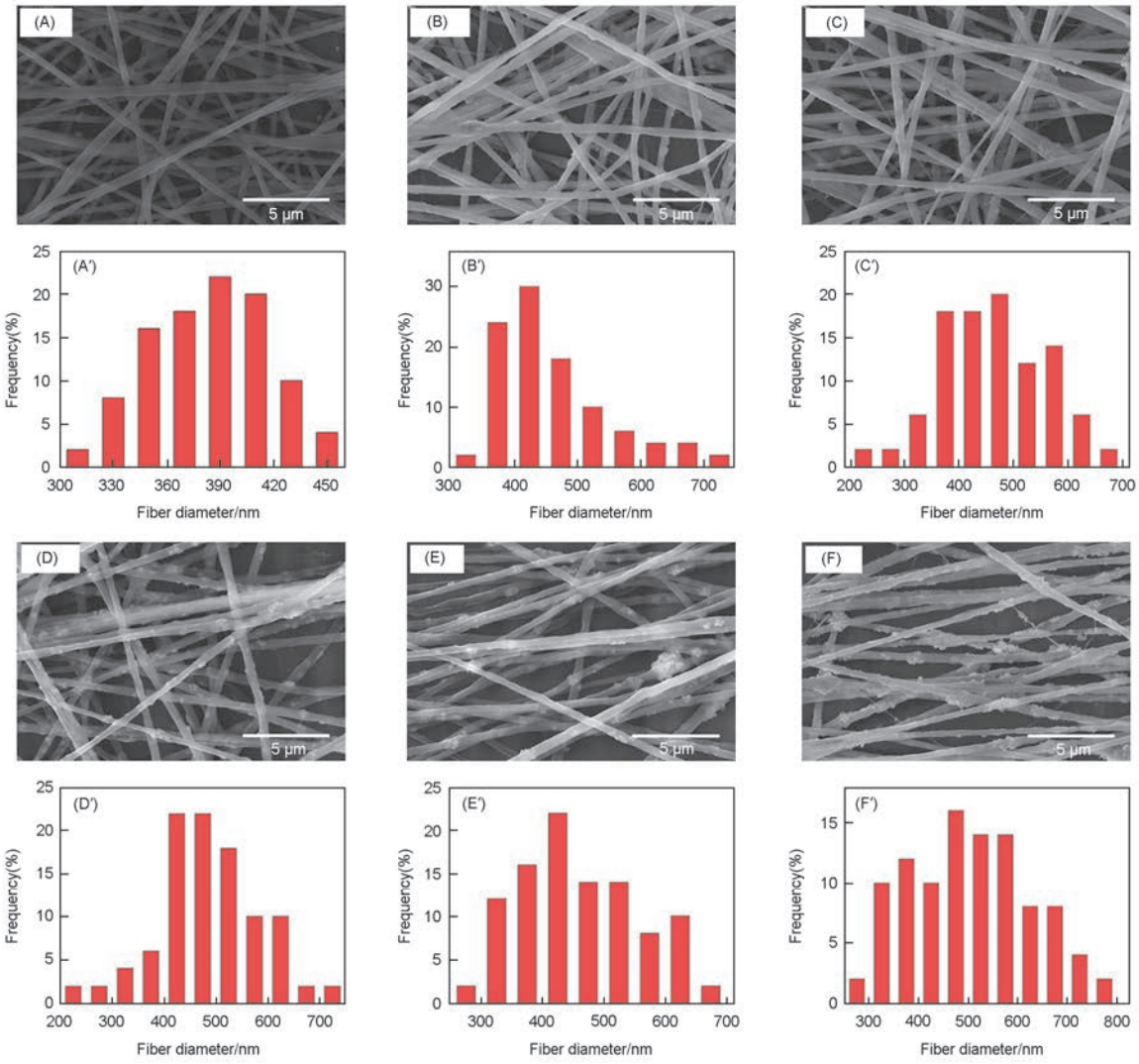

Fig.4 Typical SEM images[(A)—(F)] and nanofiber diameter distribution histogram[(A′)—(F′)] of P(A, A′), P-T^1(B, B′), P/T^1(C, C′), P/T^3(D, D′), P-T^1/T^1(E, E′) and P-T^1/T^3(F, F′) nanofiber membranes

3.2 Elements Compositions of Composite Nanofibers

EDS mapping was performed on the P, P-T^1 and P-T^1/T^3 samples to determine the presence of TiO_2 nanoparticles in the nanofibers, and the resulting EDS mappings are shown in Fig.5(A)—(C). Fig.5(B) shows that most of TiO_2 nanoparticles were imbedded inside the nanofiber and some TiO_2 nanoparticles were agglomerated. Meanwhile, the TiO_2 nanoparticles shown in Fig.5(C) were more evenly distributed, indicating that the distribution of TiO_2 can be optimized in the process of coaxial electrospinning. EDS was performed to determine the elemental compositions in the nanofibers, and the result is shown in Table 2. The content of Ti element increased to 3.81%(mass fraction)(P-T^1/T^3) by coaxial electrospinning, which was three times high than that in the

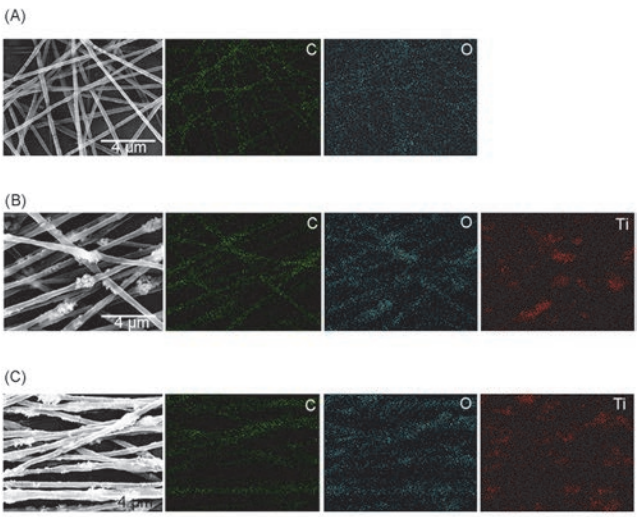

Fig.5 EDS mappings of P(A), P-T^1(B) and P-T^1/T^3(C)
Green: C; blue: O; red: Ti.

https://doi.org/10.1007/s40242-021-1118-2

Table 2 Elemental compositions of electrospinning membranes from EDS

Sample	Elemental composition as determined from EDS(%, mass fraction)		
	C	O	Ti
P	57.86	42.14	—
P-T^1	55.08	43.66	1.26
P/T^1	55.86	42.71	1.43
P/T^2	55.15	43.03	1.82
P/T^3	54.01	43.73	2.26
P-T^1/T^1	53.81	43.10	3.09
P-T^1/T^2	54.85	41.80	3.35
P-T^1/T^3	51.89	44.30	3.81

sample(P-T^1) by ordinary hybrid electrospinning. Among the samples that was made by the modified coaxial electrospinning method, with the increase of concentration of TiO_2 suspension, the content of Ti element in the membranes increased. The results of EDS agreed with the SEM results.

3.3 XRD and FTIR Analysis

XRD analyses of the TiO_2 nanoparticles, PEO nanofibers and P/T^3, P-T^1/T^3 nanofibers are shown in Fig.6. The characteristic peaks of PEO and TiO_2 nanoparticles can be clearly seen in the figures. The two distinctive peaks highlighted between 2θ=15°—25° in Fig.6(B) correspond to the amorphous PEO[30] with the diffraction range of these two characteristic peaks being 2θ=19.1° and 23.4° respectively. It can be identified through Fig.6(A) that the main characteristic peaks and the corresponding lattice planes of the rutile phase of TiO_2 nanoparticles were assigned at 2θ=27.5°(110), 36.1°(101), 39.2°(200), 41.3°(111), 44.1°(210), 54.3°(211), 56.7°(220), 62.7°(002), 64.1°(310), 69.0°(301), 69.8°(112), 76.6°(202), 79.9°(212), 82.4°(321), 84.3°(400) and 89.6°(222)[31]. While in Fig.6(C), the characteristic peaks of PEO and TiO_2 can be clearly observed, which demonstrated that both materials contain TiO_2 nanoparticles.

The FTIR spectra for P, P-T^1, P/T^3 and P-T^1/T^3 nanofiber are given in Fig.6(D). The bands of 957 and 1107 cm^{-1} correspond to the C—O group asymmetric stretching vibrations and C—O—H bending vibrations of PEO, respectively. The peaks that appear at 1340 and 1464 cm^{-1} are caused by the vibration of the CH_2— groups of PEO and the strong band near 2870 cm^{-1} is attributed to the symmetric and asymmetric C—H stretching[32]. The peak near 667 cm^{-1}, which can be clearly seen in P- T^1, P/T^3 and P-T^1/T^3 nanofibers, is claimed to correspond to the vibration of Ti—O—O bond[21].

The characteristic peak spectra of PEO and TiO_2 were observed in FTIR spectral analysis, respectively, which proved that the composite material containing TiO_2 could be prepared in the modified coaxial electrospinning way. The results indicated that the surface functionalization method was realized, which could be further applied in the preparation of surface functionalized nanofibers as PAN, cellulose, etc.

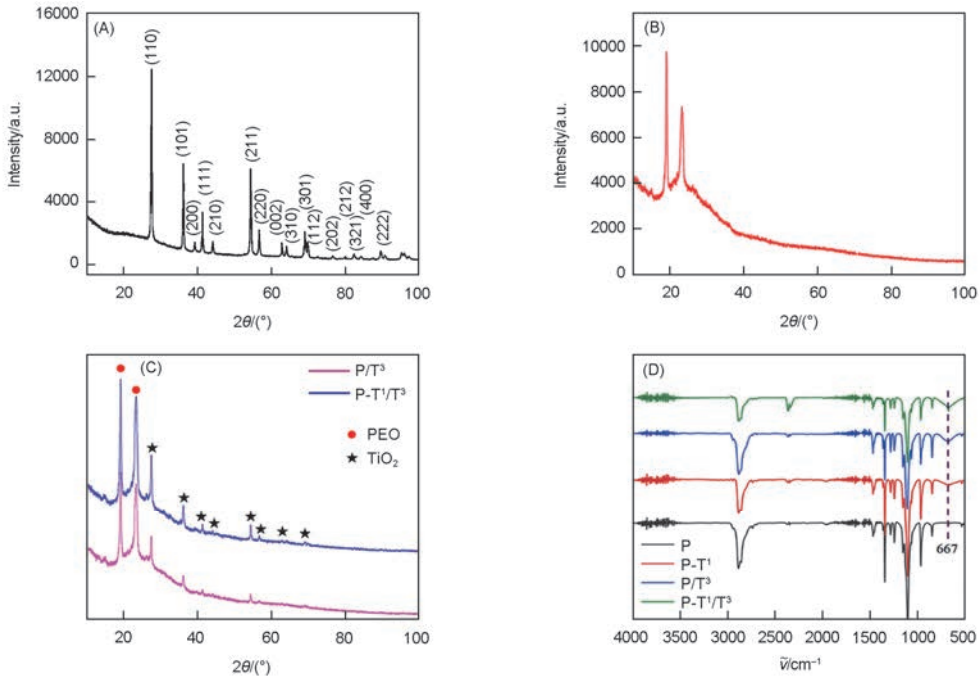

Fig.6 XRD patterns of TiO_2 nanoparticles(A), PEO nanofiber(B) and P/T^3, P-T^1/T^3 nanofibers(C), and FTIR spectra(D) of P, P-T^1, P/T^3 and P-T^1/T^3 nanofibers

https://doi.org/10.1007/s40242-021-1118-2

3.4 UV Resistance Test

The capacity of UV resistance for different membranes was quantified by UV resistance test, and the results are shown in Fig.7. With the addition of TiO_2 nanoparticles, the UV resistance of the membranes had been improved. The UV intensity received by the irradiometer in the absence of shade is 3600 μW/cm². The result of the samples by hybrid electrospinning is shown in Fig.7(A) while those of coaxial electrospinning samples are shown in Fig.7(B) and (C). It can be clearly seen that the UV resistance of electrospinning samples is improved significantly with the addition of TiO_2 nanoparticles, and the increase of TiO_2 content promotes the improvement of UV shielding performance.

After 600 s of electrospinning, the UV transmission intensity through the PEO nanofiber reduced from 3600 μW/cm² to 1555 μW/cm², while the UV transmittance of P-T^1, P/T^3 and P-T^1/T^3 nanofibers for same collecting time reached 1152, 751 and 563 μW/cm², respectively. With the addition of TiO_2 nanoparticles in the samples, the efficiencies of UV shielding of P-T^1, P/T^3 and P-T^1/T^3 nanofibers increased by 34.9%, 107.6%, and 177.9% respectively, comparing to that of the control group(PEO nanofibers). It can be concluded that the core-shell structure prepared by coaxial electrospinning plays a great role in the UV resistance.

To investigate the effect of TiO_2 on the UV resistance of nanofibers, UV-A, UV-B and UV protection factor(UPF) tests were performed on different electrospinning samples, and the results are shown in Table 3. The electrospinning time is uniformly set to 3 h. The transmittance values of UV-A and UV-B of the PEO nanofiber were high, of which the UPF reached 29.75, which basically did not have UV resistance. The UPF of hybrid P-T^1 nanofiber reached 446.51, confirming that the anti-UV properties can be improved through the surface functionalization process. Further, the samples prepared by the coaxial electrospinning process showed a significant enhancement in the anti-UV performance. The transmittance values of UV-A and UV-B of P-T^1/T^3 reduced to 0.0525% and 0.0207%, and the UPF increased to 2751.65. The experimental results indicated that the composite nanofiber membrane P/T^3 and P-T^1/T^3 were much better than the national standard.

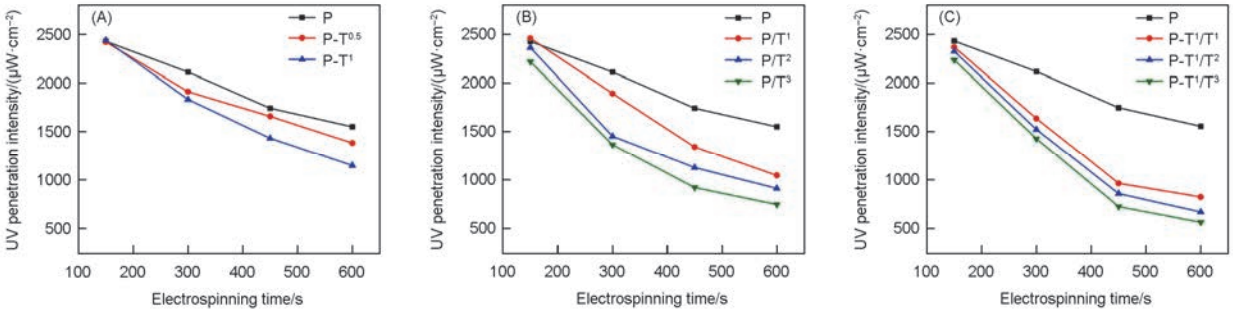

Fig.7 UV resistance of the membranes for different electrospinning time(150 s, 300 s, 450 s, 600 s)

(A) UV resistance of single spindle electrospinning sample(P, P-$T^{0.5}$, P-T^1); (B) and (C) UV resistance of the membranes of coaxial electrospinning(P/T^1, P/T^2, P/T^3, P-T^1/T^1, P-T^1/T^2, P-T^1/T^3).

Table 3 UV resistance properties of nanofibers

Sample	UV-A		UV-B		UPF
	Absorbance/a.u.	Transmittance(%)	Absorbance/a.u.	Transmittance(%)	
P	1.0079	9.8197	1.4858	3.2674	29.75
P-T^1	2.5696	0.2694	2.7658	0.1715	446.51
P/T^1	2.3111	0.4885	2.4366	0.3659	251.32
P/T^2	2.7759	0.1675	2.8896	0.1289	695.24
P/T^3	2.9452	0.1134	3.1981	0.0634	1325.48
P-T^1/T^1	2.8995	0.1260	3.0952	0.0803	1024.71
P-T^1/T^2	3.0126	0.0971	3.4965	0.0319	2433.21
P-T^1/T^3	3.2795	0.0525	3.6842	0.0207	2751.65

3.5 UV Protection Analysis

After 9 h of observation, the images of the leaf at different radiation time are shown in Fig.8. The whole leaf appeared shiny green before exposed to UV radiation. After 3 h irradiation, four dark patches appeared on the surface. This is due to the fact that UV light destroys the cellular creation of the leaf to different degrees for different parts of the leaf, consequently causing color difference between each other. The color difference gradually increased with irradiation time and finally four patches of different colors left on the leaf. The color difference between the four shielded patches suggested that P/T^3 and P-T^1/T^3 samples had better UV resistance than the

https://doi.org/10.1007/s40242-021-1118-2

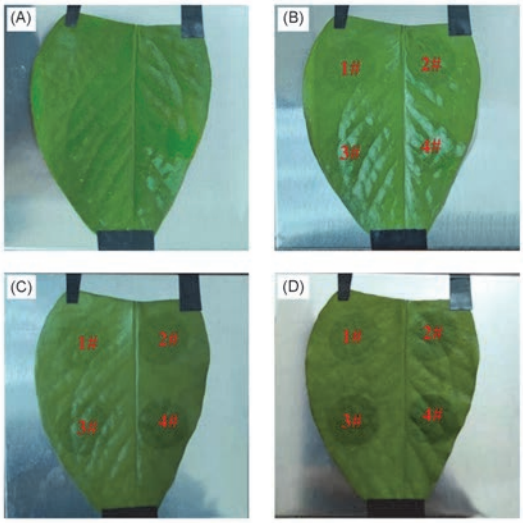

Fig.8 UV protection test with different exposing time to UV light

Time/h: (A) 0; (B) 3; (C) 6; (D) 9.

other two samples, which is in accordance to the UV resistance test described in Section **3.4**.

4 Conclusions

In this study, surface-functionalized PEO/TiO_2 composite nanofibers with excellent UV protection performance were successfully fabricated by a modified coaxial electrospinning method. The TiO_2 nanoparticles suspension was introduced into the shell channel of the coaxial spinneret, by which the contents of TiO_2 nanoparticles in the composite nanofibers can be increased and the ejection of high viscous solution can be promoted. With the content of TiO_2 increased from 0 to 3%, the average diameter of nanofibers increased from (380±30) nm to (480±100) nm. The aggregation of nanoparticles during the electrospinning was avoided, and then the TiO_2 nanoparticles dispersed evenly on the surface of composite nanofibers. Attributing to the high content of TiO_2 nanoparticles, the composite nanofiber membranes presented a superior UV resistance compared to that obtained by the conventional hybrid electrospinning. The highest UPF of the composite nanofiber was 2751.65.

Hence, the modified coaxial electrospinning for PEO/TiO_2 composite nanofibers is a good surface functionalization method for micro/nano functional materials, which could be useful in many application fields.

Acknowledgements

This work was supported by the National Natural Science Foundation of China (No.61772441), the Science and Technology Planning Project of Fujian Province, China(No.2020H6003), the Xiamen Municipal Science and Technology Project, China(No.3502Z20193015), the Fund of the Aviation Key Laboratory of Science and Technology on Inertia, China(No.20180868001) and the Fund of Fujian Innovation Center of Additive Manufacturing, China(No.ZCZZ202-31).

Conflicts of Interest

The authors declare no conflicts of interest.

References

[1] Hung C. F., Fang C. L., Al-Suwayeh S. A., Yang S. Y., Fang J. Y., *Journal of Dermatological Science*, **2012**, *68*, 135
[2] Xu Y., Sheng J., Yin X., Yu J., Ding B., *Journal of Colloid and Interface Science*, **2017**, *508*, 508
[3] Nasouri K., Shoushtari A. M., Mirzaei J., Merati A. A., *Diamond and Related Materials*, **2020**, *107*, 107896
[4] Gerber B., Mathys P., Moser M., Bressoud D., Braun-Fahrländer C., *Photochemistry and Photobiology*, **2002**, *76*, 64
[5] Fayolle B., Richaud E., Colin X., Verdu J., *Journal of Materials Science*, **2008**, *43*, 6999
[6] Li Y., Wu S., Pang L., Liu Q., Wang Z., Zhang A., *Construction and Building Materials*, **2018**, *172*, 584
[7] Li Y., Wu S., Liu Q., Dai Y., Li C., Li H., Nie S., Song W., *Construction and Building Materials*, **2019**, *220*, 637
[8] Rodriguez A. K., Mansoor B., Ayoub G., Colin X., Benzerga A. A., *Polymer Degradation and Stability*, **2020**, *180*, 109185
[9] Li F., Xu Z., Zhao K., Tang Y., *Journal of Alloys and Compounds*, **2019**, *771*, 456
[10] Yin X., Li Y., Weng P., Yu Q., Han L., Xu J., Zhou Y., Tan Y., Wang L., Wang H., *Composites Science and Technology*, **2018**, *167*, 190
[11] Wang R., Lei W., Wang L., Li Z., Chen J., Hu Z., *Chemical Research in Chinese Universities*, **2021**, *37*(3), 436
[12] San Keskin N. O., Celebioglu A., Sarioglu O. F., Uyar T., Tekinay T., *Colloids Surfaces B: Biointerfaces*, **2018**, *161*, 169
[13] Lu J., Wan H., Ju T., Ying Z., Zhang W., Li B., Zhang Y., *Journal of Alloys and Compounds*, **2019**, *774*, 593
[14] Guo X., Qin C., Huang S., Zhu M., Wang J.-J., Sun J., Dai L., *Chemical Research in Chinese Universities*, **2021**, *37*(3), 419
[15] Wang W., Wang K., He J., Zhang X., Wang C., Zhao Z., Cui F., *Chemical Research in Chinese Universities*, **2015**, *31*(6), 1012
[16] Bragaglia M., Cherubini V., Nanni F., *Composites Science and Technology*, **2020**, *199*, 108365
[17] Jiang W., Zong X., Wang X., Sun Z., *Chemical Research in Chinese Universities*, **2020**, *36*(6), 1097
[18] Pragathiswaran C., Smitha C., Mahin Abbubakkar B., Govindhan P., Anantha Krishnan N., *Materials Today: Proceedings*, **2021**, *8*, 664
[19] Hou J., Yang Y., Yu D.-G., Chen Z., Wang K., Liu Y., Williams G. R., *Chemical Engineering Journal*, **2021**, *411*, 128474
[20] Lee K., Lee S., *Journal of Applied Polymer Science*, **2012**, *124*, 4038
[21] Yu J., Pang Z., Zheng C., Zhou T., Zhang J., Zhou H., Wei Q., *Applied Surface Science*, **2019**, *470*, 84
[22] Lu Y., Ou X., Wang W., Fan J., Lv K., *Chinese Journal of Catalysis*, **2020**, *41*, 209
[23] Kim J.-H., Yasukawa A., Yonezawa S., *Materials Today: Proceedings*, **2020**, *20*, 311
[24] Löf D., Hamieau G., Zalich M., Ducher P., Kynde S., Midtgaard S. R., Parasida C. F., Arleth L., Jensen G. V., *Progress in Organic Coatings*, **2020**, *142*, 105590
[25] Jahell A., Guillermo A., Fatima P., *Data in Brief*, **2018**, *16*, 1038
[26] Moghe A. K., Gupta B. S., *Polymer Reviews*, **2008**, *48*, 353
[27] Ding Y., Dou C., Chang S., Xie Z., Yu D.G., Liu Y., Shao J., *Polymers(Basel)*, **2020**, *12*, 2034
[28] Wang M., Hou J., Yu D.-G., Li S., Zhu J., Chen Z., *Journal of Alloys and Compounds*, **2020**, *846*, 156471
[29] Zhao K., Kang S. X., Yang Y. Y., Yu D. G., *Polymers(Basel)*, **2021**, *13*, 226
[30] Zou S., Xie Y., Lv R., Na B., Tong Z., Liu H., *Polymer*, **2021**, *213*, 123303
[31] Su X., He Q., Yang Y.-E., Cheng G., Dang D., Yu L., *Diamond and Related Materials*, **2021**, *114*, 108168
[32] Basu P., Repanas A., Chatterjee A., Glasmacher B., NarendraKumar U., Manjubala I., *Materials Letters*, **2017**, *195*, 10